

Supplementary information

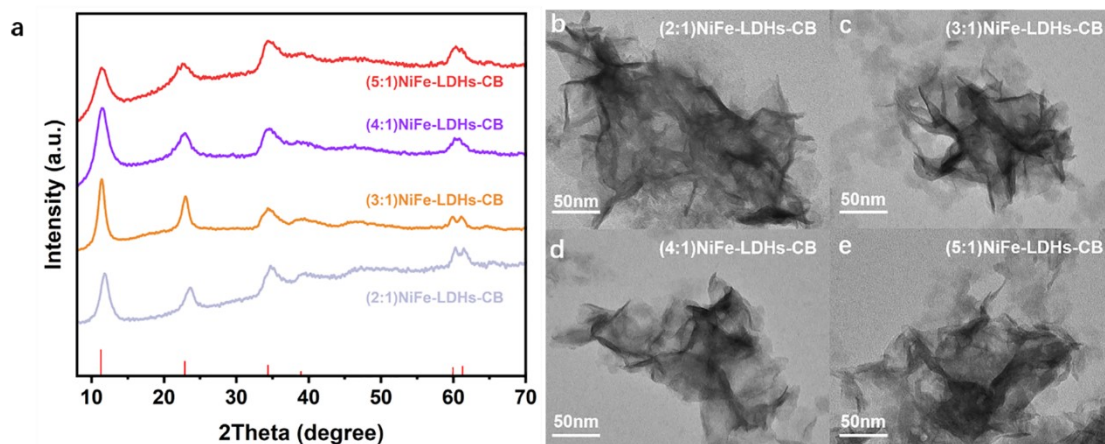


Figure S1. The crystallinity and morphology of NiFe-LDHs-CB. (a) XRD patterns and (b) morphology of the NiFe-LDHs-CB at different Ni: Fe ratios.

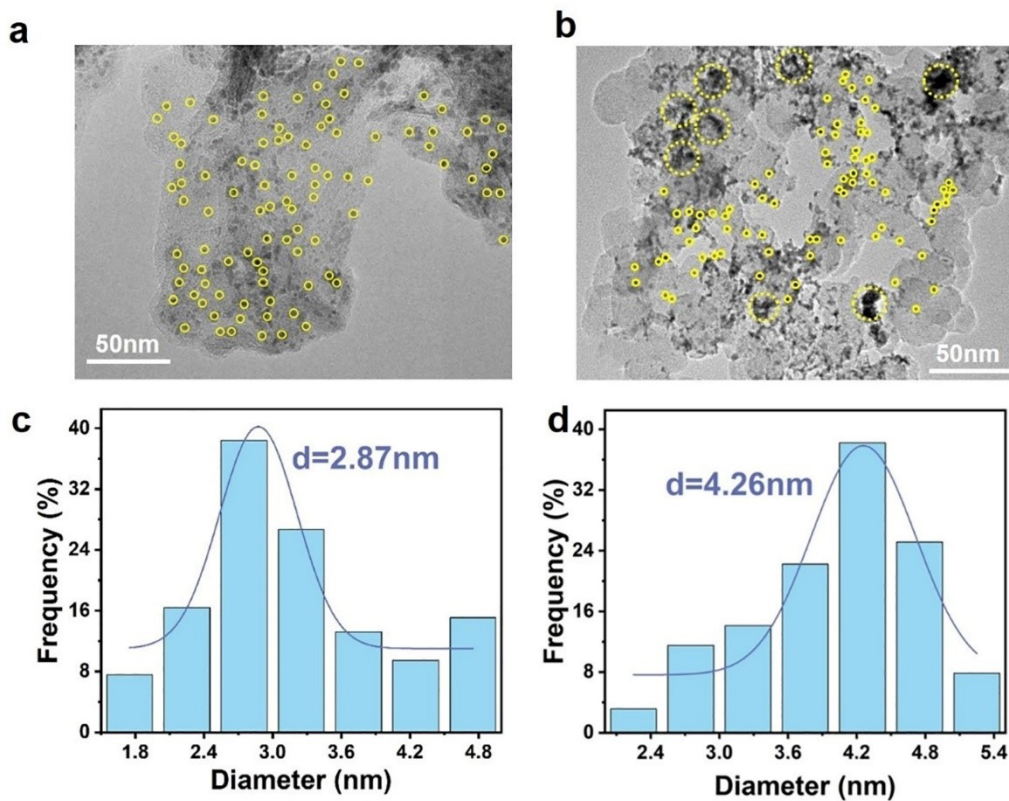


Figure S2. TEM images of (a) PtRu/NiFe-LDHs-CB and (b) commercial PtRu/C catalyst. Size distribution histograms of (c) PtRu/NiFe-LDHs-CB and (d) commercial PtRu/C catalyst.

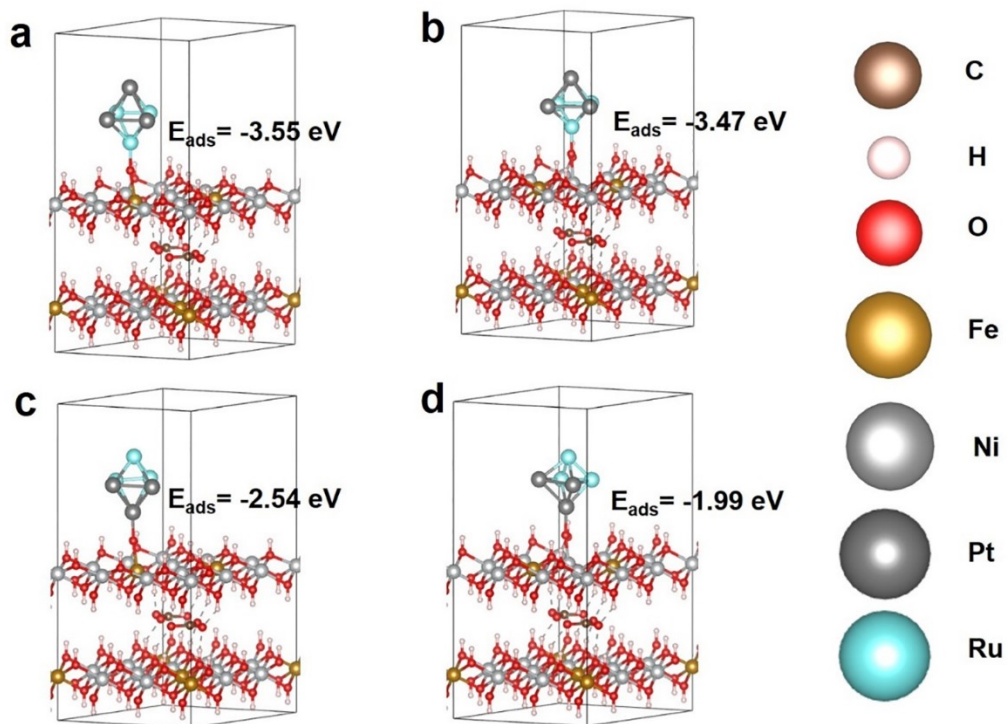


Figure S3. Comparison of adsorption energies of Ru on (a) Fe sites and (b) Ni sites; Pt on (c) Fe sites and (d) Ni sites.

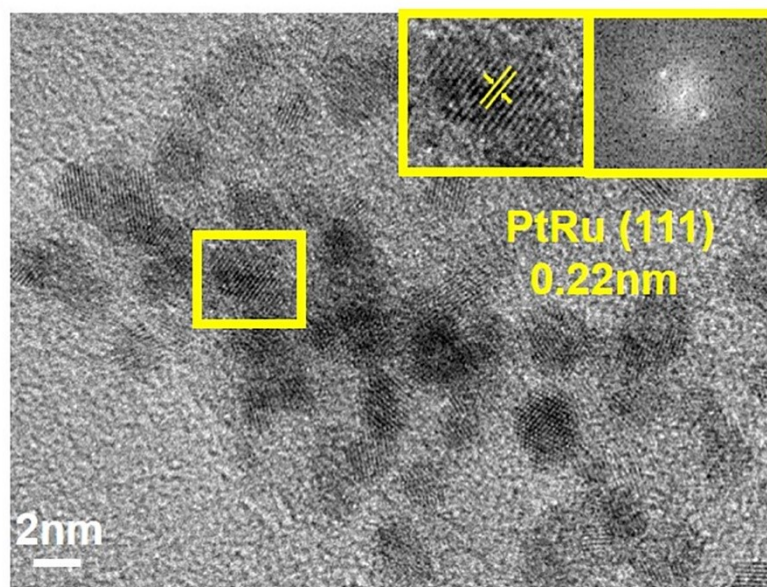


Figure S4. HRTEM images of commercial PtRu/C.

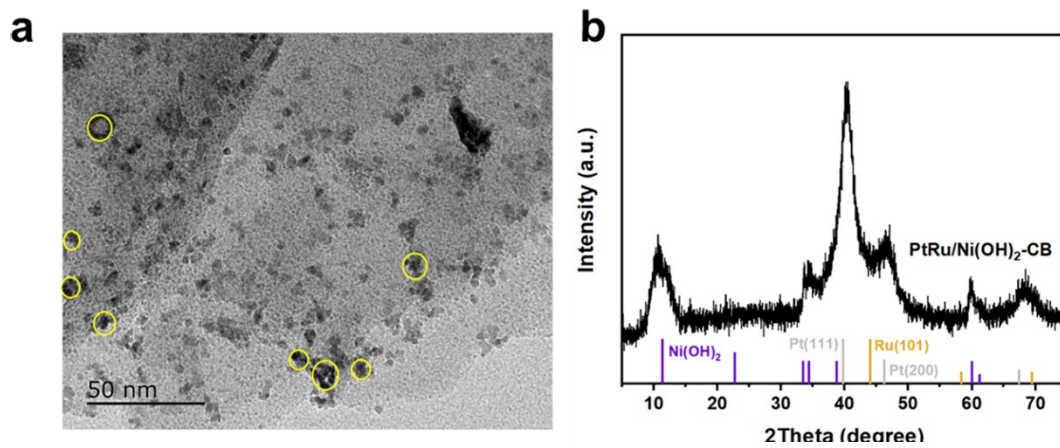


Figure S5. (a) TEM image and (b)XRD pattern of PtRu/Ni(OH)₂-CB catalyst.

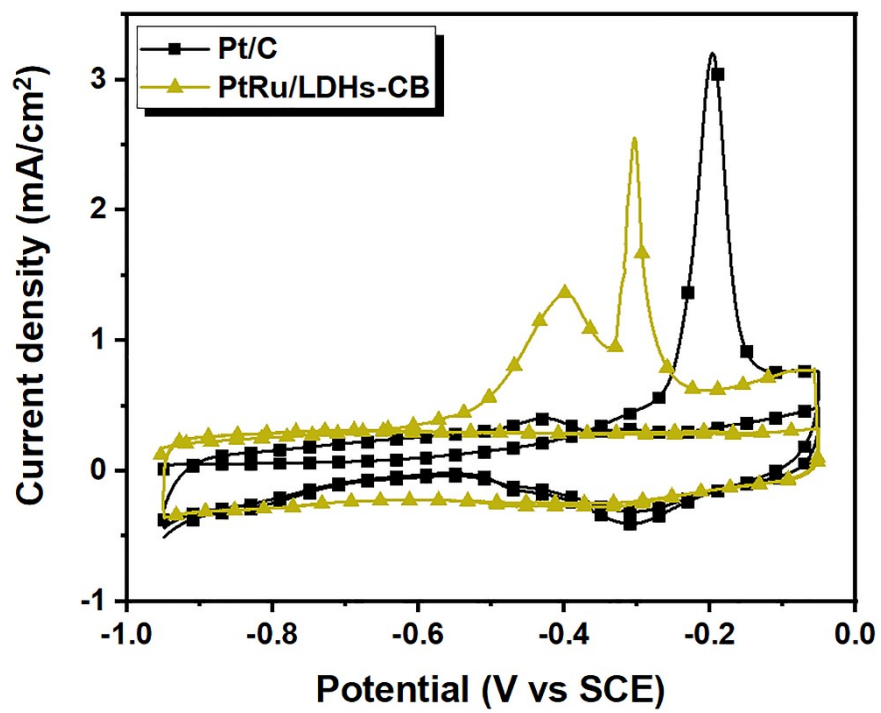


Figure S6. CO stripping of Pt/C and PtRu/NiFe-LDHs-CB.

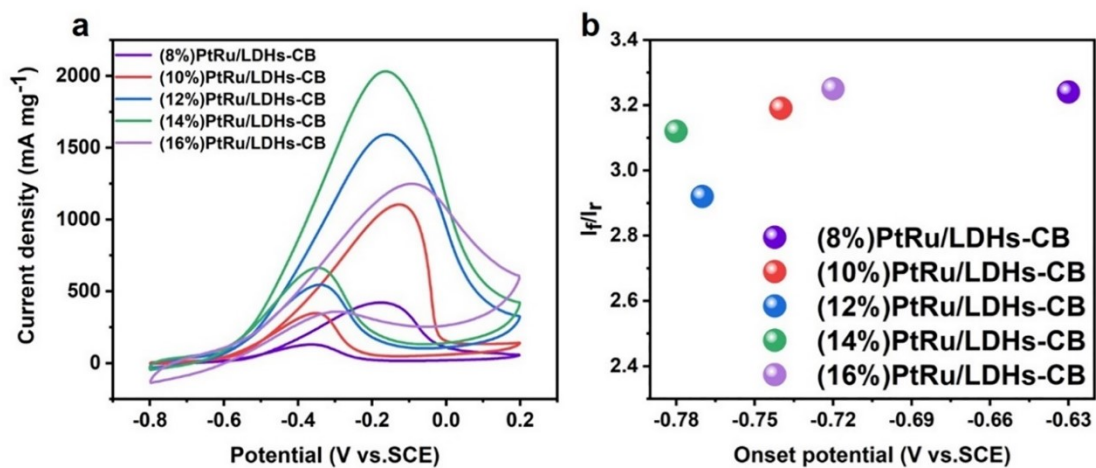


Figure S7. MOR performance summary of PtRu/NiFe-LDHs-CB with different PtRu alloy loadings.

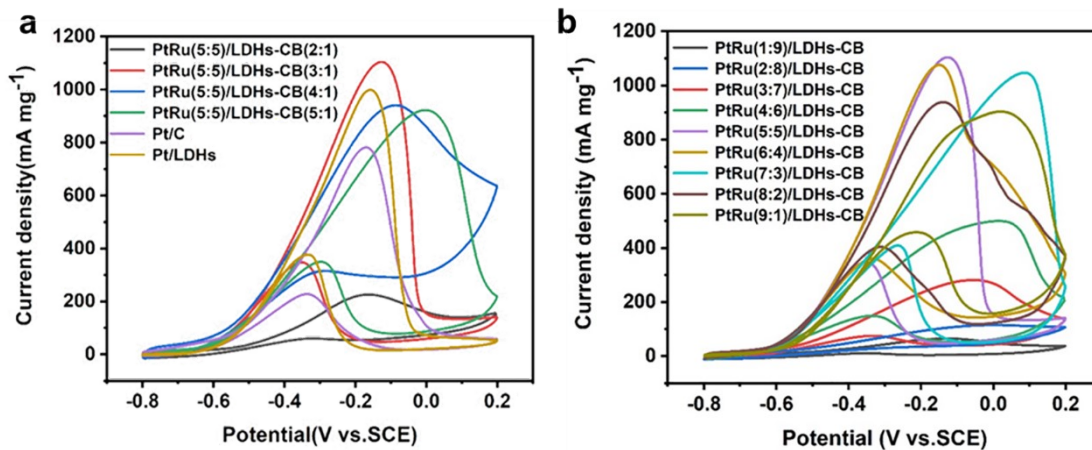


Figure S8. MOR performance summary of PtRu/NiFe-LDHs-CB with different (a) Ni: Fe ratios and (b) Pt: Ru ratios.

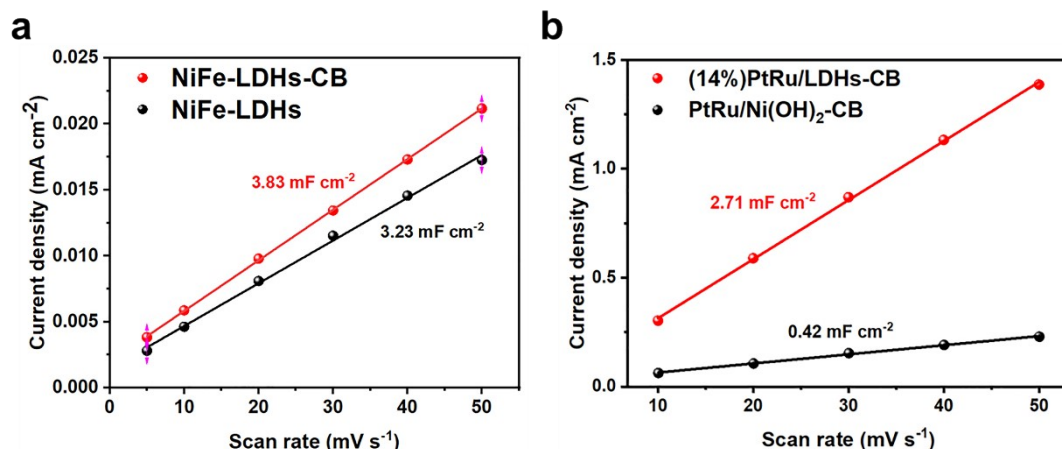


Figure S9. Change of current density plotted against the scan rate.

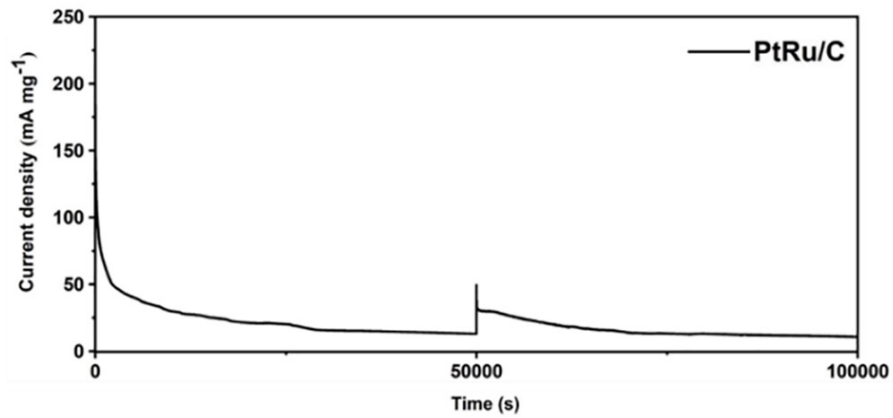


Figure S10. Long-term durability measurements of standard PtRu/C. The reaction medium was renewed every 50,000s electrocatalysis process.

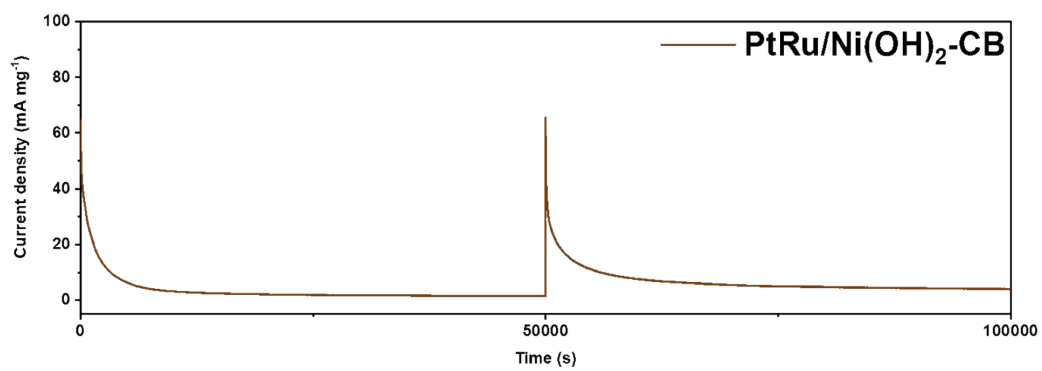


Figure S11. Long-term durability measurements of PtRu/Ni(OH)₂-CB. The reaction medium was renewed every 50,000s electrocatalysis process.

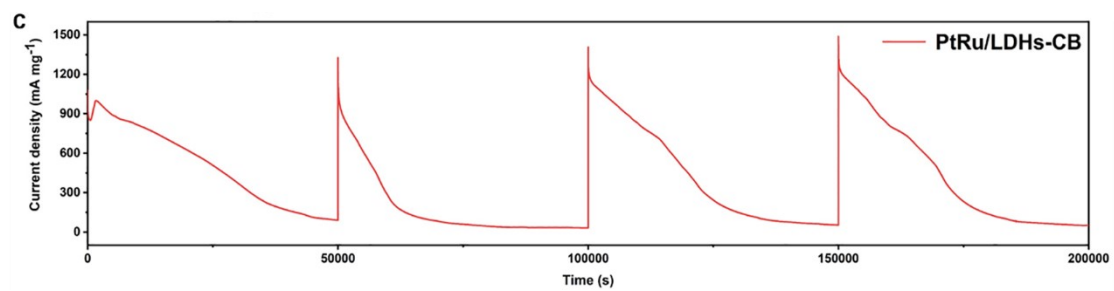


Figure S12. Long-term durability measurements of PtRu/NiFe-LDHs-CB. The reaction medium was renewed every 50,000s electrocatalysis process.

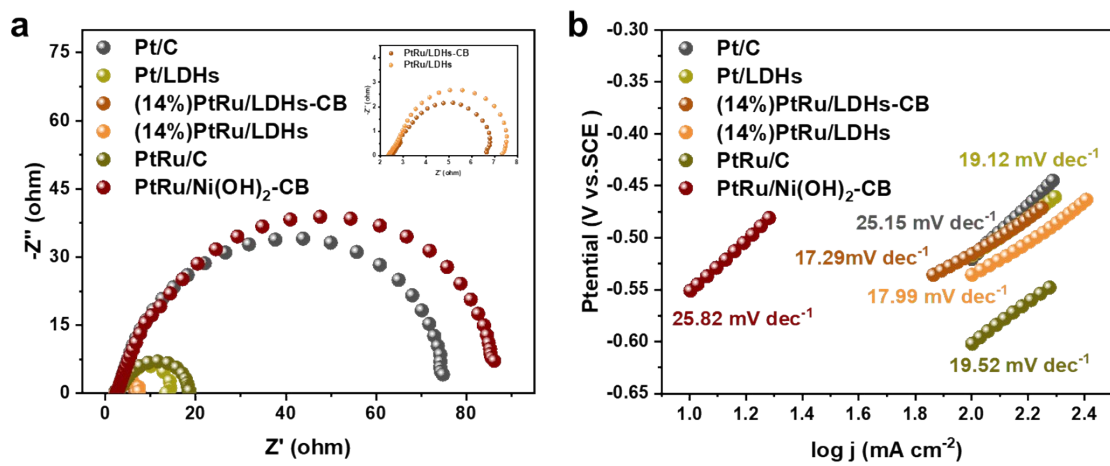


Figure S13. EIS spectrogram (a) and Tafel slopes (b) of Pt/C, Pt/LDHs, PtRu/C, PtRu/Ni(OH)₂-CB and PtRu/NiFe-LDHs-CB for MOR in 1.0 M CH₃OH and 1.0 M KOH solution.

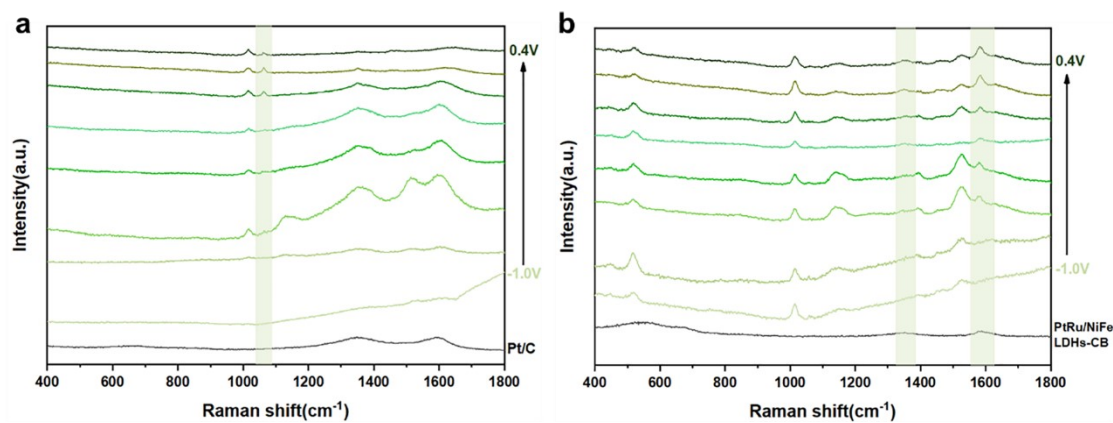


Figure S14. In situ Raman spectra of (a) Pt/C and (b) PtRu/NiFe-LDHs-CB for MOR from -1.0 V to 0.4 V (vs. Ag/AgCl) in 1.0 M CH₃OH and 1.0 M KOH solution.

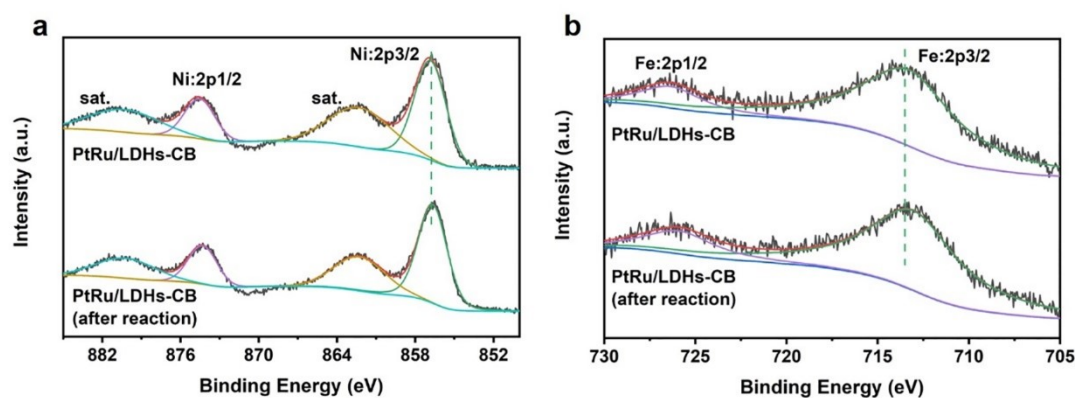


Figure S15. (a) Ni 2p and (b) Fe 2p XPS spectra of PtRu/NiFe-LDHs-CB before and after the 100,000 s chronoamperometric measurement towards MOR.

Table S1. OH adsorption energies for possible adsorption cases on NiFe-LDHs

Samples	Adsorption Energy (eV)	
	Ni: Fe=2: 1	Ni: Fe=3: 1
Ni	1.7386	1.1094
Fe	1.0707	0.9869

Table S2. Activity and stability comparison of different MOR catalysts

Catalysts	Methanol concentration	Mass activity (mA/mg _(Pt/Pd))	Activity retention value	Ref.
PtRu/LDHs-CB	1 M CH ₃ OH	2031	0.8 V/3600 s/61.54%	This work
Au/PtCu	1 M CH ₃ OH	1500	0.65 V/2000 s/13.34%	Small, 2014, 10, 3262-3265
Pt/Ni(OH) ₂ /rGo	1 M CH ₃ OH	1070	0.7 V/3600 s/90%	Nat. Commun., 2015, 6, 10035
Pt ₁ -NiO ₁	1 M CH ₃ OH	880	0.74 V/3600 s/24%	Appl. Surf. Sci., 2017, 411, 379-385
Pt-Bi/GNs	1 M CH ₃ OH	2005	0.85 V/2000 s/45%	Electrochim. Acta, 2018, 264, 53-60
Pt/GNs	1 M CH ₃ OH	504	0.85 V/2000 s/20%	Electrochim. Acta, 2018, 264, 53-60
Pt/NiFe-LDH/rGO	1 M CH ₃ OH	949.3	0.7 V/1000 s/31.6%	J. Electroanal. Chem., 2018, 818, 198-203
Pt-CoOOH-CD/C-30%	1 M CH ₃ OH	645	0.7 V/10000 s/42.7%	Mater. Chem. Phys., 2019, 225, 64-71
Pt-CoOOH-CD/C-45%	1 M CH ₃ OH	856	0.7 V/10000 s/65.24%	Mater. Chem. Phys., 2019, 225, 64-71
Pt-Ni nanooctahedra/C	1 M CH ₃ OH	1000	0.8 V/1000 s/23.8%	Chem. Eur. J., 2019, 25, 7185-7190
Pt-Ni@PANI-1	1 M CH ₃ OH	2500	0.8 V/1000 s/17.47%	Chem. Eur. J., 2019, 25, 7185-7190
Pt-Ce(CO ₃)OH/rGO-1	1 M CH ₃ OH	1277.5	0.68 V/3600 s/20.83%	J. Mater. Chem. A, 2019, 7, 6562-6571
Pt-Ce(CO ₃)OH/rGO-2	1 M CH ₃ OH	1477.5	0.68 V/3600 s/66%	J. Mater. Chem. A, 2019, 7, 6562-6571
Pt-Ce(CO ₃)OH/rGO-3	1 M CH ₃ OH	1273.7	0.68 V/3600 s/30.77%	J. Mater. Chem. A, 2019, 7, 6562-6571
IL-Pd ₃ Cu ₁	1 M CH ₃ OH	2960	0.75 V/3600 s/11.12%	Mater. Horiz., 2020, 7, 2407-2413
Pd-PdO PNTs-260	1 M CH ₃ OH	1113	0.7 V/10000 s/28.5%	Adv. Funct. Mater., 2020, 30, 2000534
S-RGO-Pt	1 M CH ₃ OH	644	0.75 V/3600 s/2.25%	Mater. Today Energy, 2021, 19, 100588
N-C/Pt	3 M CH ₃ OH	1800	0.8 V/4000 s/30%	Small, 2022, 18, 2107067

Co-N-C/Pt	3 M CH ₃ OH	5600	0.8 V/4000 s/60%	Small, 2022, 18, 2107067
Pd-UNs/Cl-GDY	1 M CH ₃ OH	3600	0.97 V/12000 s/6.7%	Angew. Chem. Int. Ed., 2023, 62, e202308968
Pt-Co@NC-850	0.5 M EtOH	5390	0.836 V/7200 s/36%	Chem. Eng. J, 2023, 473, 145028

Table S3. Power density comparison of different anode catalysts in DMFCs

Catalysts	Methanol concentration	Metal loading	Power density	Ref.
PtRu/LDHs-CB	3M CH ₃ OH	1.4 mg cm ⁻²	157 mW cm ⁻²	This work
PtRu/C	3M CH ₃ OH	1.4 mg cm ⁻²	68 mW cm ⁻²	This work
PtRu/PC-H	3M CH ₃ OH	1 mg cm ⁻²	83.7 mW cm ⁻²	Appl. Catal. B Environ. 263 (2020) 118345
PtRu/PC-L	3M CH ₃ OH	1 mg cm ⁻²	46.5 mW cm ⁻²	Appl. Catal. B Environ. 263 (2020) 118345
PtRu/C/Nafion/PVA	4M CH ₃ OH	2 mg cm ⁻²	44 mW cm ⁻²	J. Power Sources. 255 (2014) 70-75
PtRu/Porous MPL	3M CH ₃ OH	2 mg cm ⁻²	43.7 mW cm ⁻²	J. Power Sources. 262 (2014) 213-218
PtRu/C+20% IrO ₂	2M CH ₃ OH	0.82 mg cm ⁻²	23 mW cm ⁻²	Electrochim. Acta 128 (2014) 304-310
PtRuMo/CNTs	3M CH ₃ OH	2 mg cm ⁻²	61.3 mW cm ⁻²	Int. J. Hydrogen Energy 2010, 35 (2010): 8225-8233
PdFe/C	5M CH ₃ OH	1 mg cm ⁻²	42 mW cm ⁻²	Materials 10 (2017): 580-586
Pd/C-E TEK	5M CH ₃ OH	1 mg cm ⁻²	26 mW cm ⁻²	Materials 10 (2017): 580-586
Pt ₅₀ Ru ₅₀ /C E-TEK	2M CH ₃ OH	1 mg cm ⁻²	120 mW cm ⁻²	Int. J. Electrochem. Sci. 4 (2009) 954-961
IL/Pd ₃ Cu ₁	1M CH ₃ OH	2 mg cm ⁻²	8 mW cm ⁻²	Mater. Horiz. 2020, 7, 2407-2413
PtRu/C-JM	1M CH ₃ OH	2 mg cm ⁻²	27.7 mW cm ⁻²	J. Mater. Chem. A. 2017, 5, 19857-19865
Pt/pp-CeO ₂	1M CH ₃ OH	5 mg cm ⁻²	40 mW cm ⁻²	Int. J. Hydrogen Energy. 2023, 48, 5953-5960
Pt-NiTiO ₃ /C	1M CH ₃ OH	0.5 mg cm ⁻²	32.8 mW cm ⁻²	Mater Lett, 276 (2020) 128222
PtCu NWs	1M CH ₃ OH	0.6 mg cm ⁻²	49.7 mW cm ⁻²	ACS Catal. 2021, 11, 14428-14438
PtRu/C	5M CH ₃ OH	1.5 mg cm ⁻²	48.2 mW cm ⁻²	J. Power Sources. 561 (2023) 232732

Pt/C	8M CH ₃ OH	1.67 mg cm ⁻²	117.0 mW cm ⁻²	Adv. Mater. 2021, 33, 2103383
NiPt-Mo ₂ C@C	1M CH ₃ OH	5 mg cm ⁻²	45 mW cm ⁻²	Green Energy Environ 8 (2023) 559–566
Pd _{0.60} Bi _{0.35} Au _{0.05} /C	3M CH ₃ OH	1.25 mg cm ⁻²	112.4 mW cm ⁻²	Nano Res. 2022, 15(7): 6036–6044
Pd _{0.62} Bi _{0.38} /C	3M CH ₃ OH	1.25 mg cm ⁻²	87.2 mW cm ⁻²	Nano Res. 2022, 15(7): 6036–6044
